Glycobiology vol. 12 no. 11 pp. 721–727, 2002

Variant heparan sulfates synthesized in developing mouse brain differentially regulate FGF signaling

Miriam Ford-Perriss[1,3], Scott E. Guimond[1,4], Una Greferath[3], Magdalena Kita[3], Kay Grobe[5], Hiroko Habuchi[6], Koji Kimata[6], Jeffrey D. Esko[5], Mark Murphy[3], and Jeremy E. Turnbull[2,4]

[3]Department of Anatomy and Cell Biology, University of Melbourne, Victoria, Australia, 3052; [4]School of Biosciences, University of Birmingham, Edgbaston, Birmingham, B15 2TT, UK; [5]Department of Cellular and Molecular Medicine, Glycobiology Research and Training Center, University of California, San Diego, La Jolla, CA 92093-0687, USA; and [6]Institute for Molecular Science of Medicine, Aichi Medical University, Japan

Received on January 1, 2002;; revised on May 2, 2002; accepted on May 29, 2002

Heparan sulfates (HSs) exert critical regulatory actions on many proteins, including growth factors, and are essential for normal development. Variations in their specific sulfation patterns are known to regulate binding and signaling of fibroblast growth factors (FGFs) via tyrosine kinase receptors (FGFRs). We previously reported differences in sulfation patterns between HS species expressed by embryonic day 10 (E10) and E12 mouse neural precursor cells. We have examined the abilities of the different HS species to support signaling of the relevant FGF-FGFR combinations expressed early during brain development. For FGF8, which only functions early (E8–E11), E10 HS showed preferential activation. The most potent signaling for FGF8 was via FGFR3c, for which E10 HS was strongly active and E12 HS had no activity. For FGF2, which functions from E10 to E13, HS from both stages showed similar activity and were more potent at activating FGFR1c than the other receptors. Thus, we find a stage-specific correlation with activation. To explore the potential mechanisms for the generation of these stage-specific HS species, we investigated the expression of the HS sulfotransferase (HSST) isozymes responsible for creating diverse sulfation motifs in HS chains. We find that there are stage-specific combinations of HSST isozymes that could underlie the synthesis of different HS species at E10 and E12. Collectively, these data lead us to propose a model in which differential expression of HSSTs results in the synthesis of variant HS species that form functional signaling complexes with FGFs and FGFRs and orchestrate proliferation and differentiation in the developing brain.

Key words: brain development/FGF/FGF receptor/heparan sulfate/sulfotransferases

Introduction

Fibroblast growth factors (FGFs) have multiple critical roles during the formation of the central nervous system (Ford-Perriss *et al.*, 2001). FGF2 and FGF8 are particularly important in the early phases of patterning, proliferation, and neurogenesis. FGF2 regulates the proliferation of neural precursor cells (Murphy *et al.*, 1990, 1994; Qian *et al.*, 1997; Vaccarino *et al.*, 1999); studies of FGF2-null mice indicate that this factor regulates the division of precursor cells in the cerebral cortex during early neurogenesis (Raballo *et al.*, 2000). FGF8 is a key signaling molecule in establishing patterning of the brain (Crossley *et al.*, 1996; Shimamura and Rubenstein, 1997; Martinez *et al.*, 1999; Fukuchi-Shimogori and Grove, 2001). Many studies indicate that these FGFs and probably others act in a highly localized manner to regulate the development of different brain regions (Ragsdale and Grove, 2001; Ford-Perriss *et al.*, 2001). In addition, the binding of FGFs to FGF receptors (FGFRs) involves heparan sulfate proteoglycans (HSPGs) as modulatory co-receptors (Ornitz, 2000). Differences in heparan sulfate (HS) structure affect the ability of FGFs to signal through specific FGFRs (Guimond *et al.*, 1993; Guimond and Turnbull, 1999; Kan *et al.*, 1999; Pye *et al.*, 2000) and tissue-specific HS species bind FGFs differentially and regulate their recognition by FGFRs in developing mouse tissues (Allen *et al.*, 2001). Thus, HSPGs are likely to modulate FGF signaling in the developing brain.

HSs are complex sulfated polysaccharides that contain polymorphic sulfated sequence motifs that are responsible for numerous protein binding and regulatory properties. HS chains are attached to core proteins to form HSPGs, which are known to have diverse biological functions (Bernfield *et al.*, 1999), and recent genetic studies have provided compelling evidence that they are essential for normal development (Lander and Selleck, 2000). HS chains are produced by a complex biosynthetic process that generates diverse molecular motifs with unique displays of sulfate, carboxyl, and hydroxyl groups (Lindahl *et al.*, 1998; Turnbull *et al.*, 2001). Sulfation requires a family of HS sulfotransferases (HSSTs) including four N-deacetylase-N-sulfotransferases (NDSTs; Aikawa *et al.*, 2001), three 6-O-sulfotransferases (6-OSTs; Habuchi *et al.*, 2000), at least five 3-OSTs; Shworak *et al.*, 1999) and a single 2-OST (Kobayashi *et al.*, 1997). These HSSTs have different substrate specificities and can generate different structural motifs (Aikawa *et al.*, 2001; Habuchi *et al.*, 2000; Liu *et al.*, 1999). Mice lacking specific HSSTs have severe phenotypes with numerous developmental defects (Bullock *et al.*, 1998; Forsberg *et al.*, 1999; Humphries *et al.*, 1999; Ringvall *et al.*, 2000). Thus, the isozyme diversity of HSSTs may be critical for generating differing sequence repertoires in HS chains.

[1]These authors contributed equally to this work.

[2]To whom correspondence should be addressed; E-mail: j.e.turnbull@bham.ac.uk

In an earlier study we compared the structure of HS from primary cultures of neural precursor cells isolated at a mainly proliferative phase, embryonic day 10 (E10), and one where neuronal differentiation begins (E12). HS from E12 cells had longer chains with more sulfated domains, a higher level of 2-O-sulfation, and altered patterns of 6-O-sulfation and N-sulfation relative to the E10 HS (Brickman *et al.*, 1998a,b). In this article we describe studies to determine the relative abilities of the E10 and E12 HS to activate FGF signaling through relevant receptors and to relate this to the expression levels of HSSTs in developing brain. We find that they display distinct abilities to specifically activate FGF-FGFR signaling complexes relevant to brain development, and that these changes correlate with HSST expression profiles, which vary actively both *in vitro* and *in vivo*.

Results and discussion

FGFR b and c splice variants are expressed in the developing neuroepithelium

In previous studies we observed differences in fine structure of HS produced by primary cultures of neural precursor (Nep) cells (Brickman *et al.*, 1998a,b; see details already described). To relate these differences to the potential function of HS as a regulator of FGF signaling in developing brain, we first investigated expression of the FGFRs. The relative abundance of the b and c splice variants for each FGFR was determined using exon-specific primers and semi-quantitative reverse transcription polymerase chain reaction (RT-PCR). All four receptors are expressed in the developing neuroepithelium. The c splice variants for FGFR1, -2, and -3 are the most abundant at all developmental stages (Figure 1). The levels of expression are similar within and between the different receptor types at the different stages. FGFR1b expression is not detectable, levels of FGFR2b are 500-fold lower than those for FGFR2c, and FGFR3b some 50- to 100-fold lower than the expression levels of FGFR3c. FGFR4c is not detectable at E10 and is expressed at very low levels at E12 and E14 (approximately 100–200-fold lower than the other FGFR c splice variants). These data show that the c splice variant forms of FGFR1, -2, and -3 are the most abundant at E10, E12, and E14, implicating them as candidates for transduction of FGF signaling in early brain development. Other expression studies conducted in our laboratory using ribonuclease protection assay and FGFR b and c exon-specific probes also gave similar results for relative expression at E10 and E12 (data not shown) to those obtained here using RT-PCR. These results are consistent with data showing that FGFR3c is abundant in the developing neural tube (Wuechner *et al.*, 1996) and extend a previous report of FGFR1 and -2 expression in the neural tube at this time, in which splice variants and abundance were not determined (Orr-Urtreger *et al.*, 1991).

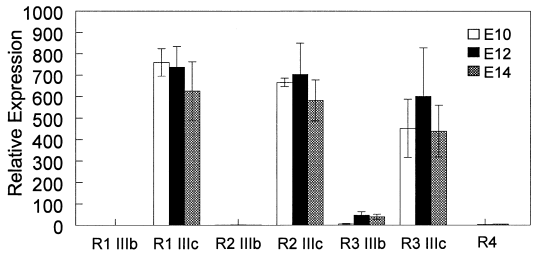

Fig. 1. FGFR1, -2, and -3 c splice variants are the most abundantly expressed FGFRs in the developing brain. Semi-quantitative RT-PCR was used as described in *Materials and methods* to quantify the expression of all four FGFRs, including both b and c splice variants, in E10, E12, and E14 neuroepithelium.

Variant Nep cell HS species regulate signaling by specific FGF-FGFR complexes

Because FGF2 and FGF8 are known to play important roles in early brain development, we next examined the ability of the embryonic brain HS to regulate their signaling in combination with relevant FGFRs. As it is not feasible to obtain sufficient *in vivo* HS from early neural tube, we used the structurally characterized HS purified from the Nep cells isolated from E10 and E12 mouse embryos and cultured for 2 days ($E10^{+2}$ and $E12^{+2}$). Their ability to activate FGF2 and FGF8 was examined using BaF3 cell lines expressing the c splice forms of FGFR1, -2, and -3. HS from both stages show similar abilities to activate FGF2 signaling via FGFR1c, FGFR2c, and FGFR3c (Figure 2A, C, and E), with both HS species more potent at activating FGFR1c than the other receptors. In marked contrast, $E10^{+2}$ HS was a potent activator of FGF8 signaling via FGFR3c (activity almost equivalent to a heparin control), and $E12^{+2}$ HS was essentially inactive (Figure 2F). Neither HS species nor a heparin control were able to activate FGF8 through FGFR1c (Figure 2B), in agreement with previous data that FGFR1c is not a receptor for this ligand (Ornitz *et al.*, 1996). Both HS species also weakly activated FGF8 signaling through FGFR2c (Figure 2D). These data indicate significant differences in the functional ability of HS species produced at different times during neuroepithelial differentiation.

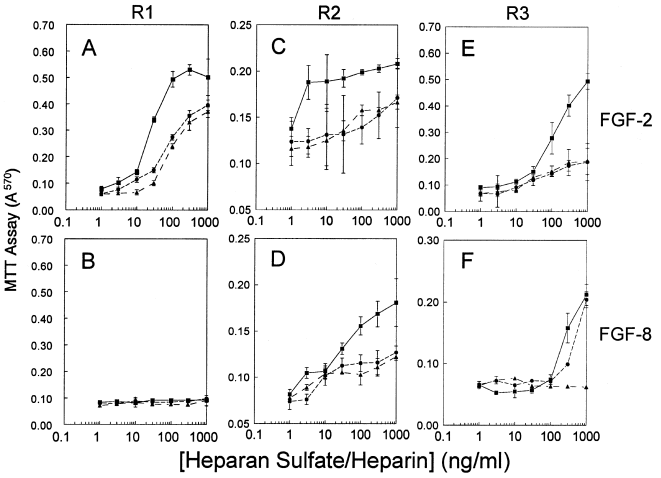

Fig. 2. HS from different stages of neuroepithelial development have different abilities to activate specific FGF-FGFR signaling complexes. HS was purified from Nep cells cultured from E10 or E12 mouse neuroepithelia. BaF3 cells expressing either FGFR1c (**A** and **B**), FGFR2c (**C** and **D**), or FGFR3c (**E** and **F**) were incubated with FGF2 (**A**, **C**, and **E**) or FGF8 (**B**, **D**, and **F**) and different concentrations of either heparin (squares), E10 HS (circles), or E12 HS (triangles). An MTT assay was used to measure resulting cell numbers.

In vitro *Nep cells exhibit stage-dependent variations in HSST RNA expression profiles*

To explore potential mechanisms for generation of the differences in structure and signaling capacities of the HS species, the expression profiles of HSST RNAs were examined. We initially assessed expression of O-sulfotransferases (OSTs) in the primary cultures of Nep cells by RT-PCR, using primers specific for the murine forms of 2-OST and three 6-OSTs (1–3). It is apparent that 2-OST, 6-OST1, and 6-OST2 are strongly expressed in both the $E10^{+2}$ and $E12^{+2}$ cultures and, importantly, that an additional 6-OST isozyme, 6-OST3, is only expressed by the more mature $E12^{+2}$ culture (Figure 3A).

To assess the expression of the NDST isozymes, primers specific for the murine forms of the four NDSTs (1–4) were used in RT-PCR (Figure 3B). In the $E10^{+2}$ cells it is apparent that only NDST2 and NDST3 are expressed, with NDST3 expression apparently the strongest. The profile differs in the more mature $E12^{+2}$ cells where NDST1 is now strongly expressed, along with NDST4 and weak NDST2 expression, whereas NDST3 is absent. Together with the OST data, these results clearly indicate development stage-dependent variations in the expression profiles of both OSTs and NDSTs *in vitro*.

We next determined the expression levels of the OSTs quantitatively in Nep cells using real-time PCR. Quantification of the abundance of the OST RNAs in these cells show that 2-OST RNA is the most abundant; from $E10^{+2}$ to $E12^{+2}$ its level increases fourfold (Figure 4A, $p < 0.005$). These levels are high and comparable to actin RNA levels (95% for $E10^{+2}$ and 40% for $E12^{+2}$ respectively; data not shown). The 6-OST RNAs also show increases in $E12^{+2}$ compared to $E10^{+2}$ cultures: for 6-OST1 RNA it is about twofold (Figure 4A; $p < 0.005$) and for 6-OST2 RNA it is about fourfold ($p < 0.01$). The levels of 6-OST1 RNA are higher than 6-OST2, and 6-OST3 RNA is only expressed by the $E12^{+2}$ cells. This quantitative data is in good agreement with the relative intensity of the standard RT-PCR bands.

HSST RNA expression profiles exhibit stage-dependent variations in developing brain

The differential expression profiles in Nep cells raised the question as to whether similar alterations occur *in vivo*. Placing cells in tissue culture in the absence of normal developmental cues could cause changes in HS biosynthesis. To address this issue, we first examined the expression of OSTs in the developing brain at E10, E12, and E14 using RT-PCR (Figure 5A). 2-OST, 6-OST1, and 6-OST2 are expressed at all stages studied. In contrast, 6-OST3 expression is absent or very weak at E10 and E12 but strongly expressed at E14. RT-PCR analysis of the expression of NDST isozymes in the developing brain (Figure 5B) show that at all three stages NDST1 are consistently expressed, whereas NDST2 is absent. NDST3 RNA is apparently expressed weakly at E10, whereas NDST4 is absent; both are expressed strongly at E12 and moderately at E14.

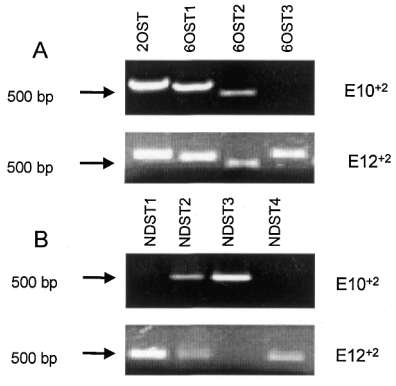

Fig. 3. HSST are differentially expressed in Nep cell cultures. Primers specific for HSSTs were used to determine mRNA expression in Nep cells. RNA purified from Nep cells cultured from E10 or E12 was examined for HSST expression using standard RT-PCR. (**A**) Expression of 2-OST and 6-OST1–3; (**B**) expression of NDST1–4.

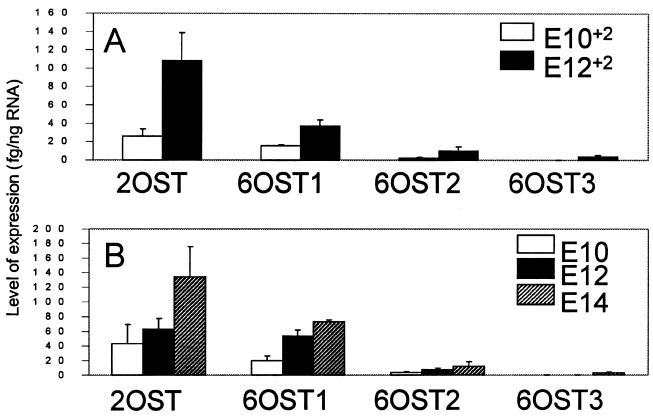

Fig. 4. Quantitative RT-PCR of OST mRNAs in neural precursor cells and in the developing brain. Primers specific for OSTs were used to determine mRNA expression in Nep cells. RNA purified from (**A**) Nep cells cultured from E10 or E12 neuroepithelium or (**B**) directly from neuroepithelia of E10, E12, or E14 mice was examined for expression of 2-OST and 6-OST1–3 quantitative RT-PCR as described in *Materials and methods*.

We also conducted real-time quantitative PCR for OSTs in the developing brain. 2-OST is the most abundant of the OSTs at each developmental stage investigated (Figure 4B). From E10 to E14, the level of 2-OST increases threefold ($p < 0.025$). These represent high expression levels similar to actin in the same tissue, as seen with the Nep cells (82.5% and 71% at E10 and E12, respectively; data not shown). Of the three 6-OST isozymes, 6-OST1 RNA expression levels are the highest, followed by 6-OST2 and then 6-OST3, which is not detected until E14 (Figure 4B). From E10 to E14 the relative abundance of 6-OST1 RNA increases about threefold ($p < 0.05$), whereas 6-OST2 RNA increases about fourfold. Again, these results are in good agreement with the standard RT-PCR data (Figure 5A) and show that the dominant OSTs are 2-OST and 6-OST1, which are expressed at similar levels. Overall, these data on OST RNA expression indicate increasing levels and altered expression profiles of these enzymes during early brain development.

It is interesting to compare the expression of HSSTs in the primary Nep cells with their counterparts *in vivo*. The OST profiles obtained from the $E10^{+2}$ and $E12^{+2}$ cultures are very similar to those obtained from the E10 and E12/E14 neuroepithelium, respectively (Figures 3A and 5A), as are the absolute levels of each (Figure 4A, B). Thus, there is a close correspondence between the relative expression and absolute levels of the OSTs *in vivo* compared with *in vitro*. However, the

NDST expression patterns exhibit both similarities and differences. At the earlier developmental ages (compare $E10^{+2}$ to E10 and E12 *in vivo*) the expression of NDST3 and NDST4 are similar *in vivo* compared with *in vitro*. At the later developmental ages (compare $E12^{+2}$ to E12 and E14 *in vivo*) the expression of NDSTs 1 and 4 are similar *in vivo* compared with *in vitro*. Differences in expression are evident for NDST1 and -2 at the early stages and for NDST2 and NDST3 in the later stages. It is possible that the NDSTs are more susceptible than are OSTs to modulation of expression in response to altered cell environment.

Significance of differential HSST isozyme expression profiles in brain development

Overall these data demonstrate that the array of HSSTs expressed varies actively in developing neuroepithelial cells both *in vitro* and *in vivo*. For both the OSTs and NDSTs, the range of expressed isozymes available increases as the embryonic brain develops and correlates temporally with increasing neuronal differentiation (Caviness *et al.*, 1995). Most important, we observed the expression of development stage-specific combinations of 6-OST and NDST isozymes.

In our earlier study of the structure of the HS from E10 and E12 neural precursor cells *in vitro*, we showed that the E12 HS had longer chains with a greater number of sulfated domains in comparison with the E10 HS. Although there were basic similarities in domain structure, distinct O-sulfation patterns were imposed on these domains. The difference in fine structure within the sulfated domains showed there was a higher level of 2-O sulfation and altered patterns of 6-O-sulfation and N-sulfation in the E12 HS chains in comparison to the E10 HS. Our current data is consistent with this in that we find a distinct elevation in the levels of expression of the 2-OSTs and 6-OSTs and an increasing complexity in the array of 6-OSTs expressed at the later stages. With respect to the NDSTs, there is a somewhat different trend between what we find *in vivo* compared with *in vitro* analyses. Because our earlier study analyzed HS from Nep cells *in vitro*, our *in vitro* data is the appropriate comparison here. We find increased levels of NDSTs 1 and 4 and decreasing levels of NDSTs 2 and 3 in E12 compared with E10 cultures. This is also consistent with our findings of altered patterns of N-sulfation between E10 and E12.

We suggest that these altered isozyme expression patterns would likely result in altered activity profiles of unique arrays of HSSTs; because the latter display different substrate specificities and product structures (Habuchi *et al.*, 2000; Aikawa *et al.*, 2001) this could underly the observed generation of different HS structures. This leads us to propose a model in which differential expression of HSSTs results in the synthesis of variant HS species that form functional signaling complexes with FGFs and FGFRs (Figure 6). It is not yet known what specific structural characteristics of the E10 and E12 HS species are responsible for the activity differences. We speculate that variations in the repertoires of specific sequences present in the two pools of chains underlie their altered abilities to productively form ternary complexes with particular FGF-FGFR combinations. Further studies will be required to isolate and elucidate the structures of these specific functional sequences.

To our knowledge this study offers the first evidence correlating specific changes in HS fine structure and bioactivities with altered expression profiles of HSSTs. It seems very likely

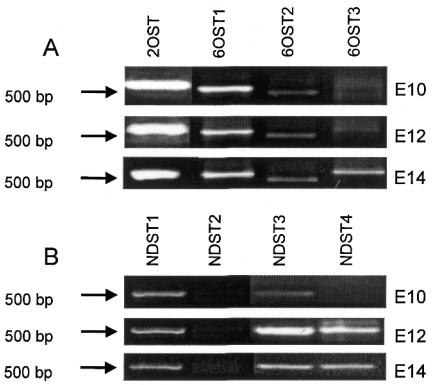

Fig. 5. HSSTs are differentially expressed in the developing brain. Primers specific for HSSTs were used to determine mRNA expression in developing mouse brain. RNA purified from neuroepithelia of E10, E12, or E14 mice was examined for for HSST expression using standard RT-PCR. (**A**) Expression of 2-OST and 6-OST1–3; (**B**) expression of NDST1–4.

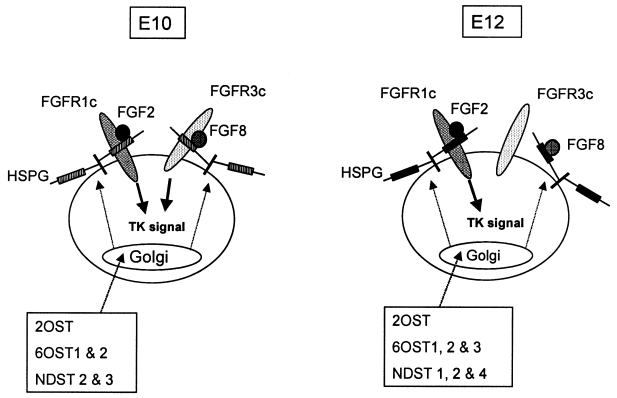

Fig. 6. A model for the dynamic biosynthetic generation of structurally and functionally variant HS species expressed during neurogenesis. Different arrays of OST and NDST isozymes expressed in the Golgi at specific developmental stages result in biosynthesis of variant HS species which are structurally distinct (Aikawa, 2001a) and display altered abilities to activate signaling of FGF2 and FGF8 via FGFR1c and FGFR3c receptor tyrosine kinases, respectively. This may provide a mechanism for dynamic generation of variant neural precursor cell HS species that actively regulate signaling by specific FGF-FGFR complexes and thus play a role in orchestrating proliferative and differentiative events during neurogenesis. The observed signaling specificity is consistent with the known temporal roles of FGF2 and FGF8 *in vivo*. E10 HS activates both FGF2/FGFR1c and FGF8/FGFR3c, whereas E12 HS only activates FGF2/FGFR1c. E12 HS may not contain appropriate specific sequences to support signaling by FGFR3c, although it must bind FGF8 because it will activate FGF8 signaling via FGFR2c. It is possible that E12 HS does not bind to FGFR3c (as shown in the diagram) or, alternatively, that it binds the receptor but does not permit formation of a ternary complex of FGFR3c with FGF8.

that the latter would impact significantly on the HS structures biosynthesized, as suggested by data on differences in HS structure due to overexpression of NDST1 or NDST2 (Pikas *et al.*, 2000). However, it remains for a relationship to protein levels to be established when specific antibodies become available, and additional mechanisms seem certain to be involved in control of HS biosynthesis. For example, we have evidence that 5′ untranslated regions of NDSTs contain regulatory elements that affect their translation (Grobe and Esko, 2002).

These results clearly demonstrate FGF signaling specificity of two structurally distinct HS species produced by Nep cells *in vitro* that display different HSST expression profiles. It is plausible that the altered HSST profiles observed *in vivo* also result in biosynthesis of distinct HS species that could regulate activation of specific FGF-FGFR signaling complexes during brain development. Our HS preparations were derived from Nep cells *in vitro*, which display some differences in NDST expression compared with *in vivo* patterns. We do not yet know whether the latter differences are conservative with respect to synthesis of specific sequences. However, the bioactivity data we obtain with these *in vitro* HS species are consistent with similar potential roles for *in vivo* HS, and our observations align closely with the time of action of FGF2 and -8 in the developing brain.

FGF8 acts mostly prior to E12, and FGF2 acts in cortical development mainly from E10 to E14 (Fukuchi-Shimogori and Grove, 2001; Raballo *et al.*, 2000; see Ford-Perriss *et al.*, 2001). In addition, the presence of spatially specific HS species that regulate FGF-FGFR recognition has recently been described in developing mouse tissues (Allen *et al.*, 2001). The synthesis of these HS species may also depend on differences in the spatial localization of HSSTs. Using *in situ* hybridization we have evidence of differences in spatial expression of 6-OST1, 6-OST2, and 6-OST3 transcripts in distinct areas of the developing mouse brain (Drummond *et al.*, unpublished data). Further investigation of *in vivo* spatiotemporal HSST expression patterns and their correlation with HS structures produced will reveal important information about the regulatory roles of HS in development.

Materials and methods

Neuroepithelium dissection, in vitro *culture, and total RNA preparation.*

Neural tubes consisting of the forebrain to midbrain (through to the midbrain/hindbrain border) were dissected at E14, E12, and E10 (Murphy *et al.*, 1990; ~1, 10–15, and 20–25 embryos, respectively, for each preparation). For cell culture, single cell suspensions of Nep cells were prepared from neural tubes as described (Murphy *et al.*, 1990). Cells were plated at 2.5×10^5 per ml in Neurobasal media (Invitrogen) in 12-well plates (Nunc) coated with 0.5 mg/ml poly-ornithine (Sigma) and 20 µg/ml laminin (Invitrogen). Cells were cultured for 48 h (about two rounds of cell division) with 10 ng/ml bovine recombinant FGF2 (Boehringer Mannheim) to produce $E10^{+2}$ and $E12^{+2}$ cultures. Total RNA was prepared from either neural tubes or cell cultures according to manufacturers instructions using Trizol™ (Invitrogen) and treated with DNAfree (Ambion) to remove residual genomic DNA. RNA was quantified by sensitive fluorescent assay using a Ribogreen RNA quantitation Kit (Molecular Probes).

RT-PCR

RT-PCR was performed on total RNA using One-Step RT-PCR (Invitrogen) according to the manufacturer's instructions (1 µg total RNA mixed with 0.5 µg each of forward and reverse primers). Primers for NDST1–4 were as described elsewhere (Aikawa *et al.*, 2001) and primers were designed for 2-OST and isozyme-specific primers for 6-OST1–3. Typical RT-PCR consisted of the following steps: 1 cycle of 94°C for 5 min and 42°C for 30 min, followed by 35 cycles of 94°C for 30 s, 50°C for 30 s, and 72°C for 45 s with a final extension of 72°C for 10 min. Primers for the 2-OST and 6-OST1–3 were as follows:

- 2-OST FP1: ATTAAGGAGACGGAAACAAGGAG;
- 2-OST RP1: GAAGGGTGGTGACACAGTCAAG;
- 6-OST1 FP1: ACCAGCAACTCTTTCTATCCC;
- 6-OST1 RP1: AGCAATACCCACCAGCATC;
- 6-OST2 FP1: TCCTTCAGACCCATTTCC;
- 6-OST2 RP1: CCCACACACAGCATAACAC;
- 6-OST3 FP1: TGAATGAGAGCGAGCGGAAC;
- 6-OST3 RP1: TGGATTGGAAATGAAGGCAGAG.

Each experiment was performed at least twice on at least two independent RNA preparations, and figures show representative examples.

Real-time quantitative PCR of OSTs

The reverse transcription step was carried out according to manufacturer's instructions using the SuperscriptII™ Preamplification system (Invitrogen) except that 50 ng of total RNA was used in a 10-µl total reaction volume. Triplicate 2-µl samples of this cDNA were quantified by real-time PCR using a Corbett RG-2000 (Corbett, Sydney, Australia) using the parameters detailed in Table I. Three to four independent dissections or cell culture experiments were analyzed, and triplicate real-time measurements were performed for each cDNA preparation. Data were analyzed using the RG-2000 quantification and melt analysis programs. Reactions were performed in a 20 µl volume: 2 µl of cDNA (from a typical RT-PCR reaction as described) and 18 µl of a master mix containing 0.2 U Taq polymerase (Fisher Biotech), buffer, 0.5 µM forward and reverse primers, $MgCl_2$ optimized at either 2 mM or 3 mM (see Table I) and 0.5× SYBR Green (Molecular Probes). A typical protocol was 1 min at 94°C (one cycle), 15 s at 94°C, 20 s at 55°C, 30 s (2-OST, 6-OST3) and 20 s (6-OST1, 6-OST2) at 72°C, 10 s at 87°C (for detection of the fluorescent product) for 35 cycles. Some additional primers were used and compared with those used for standard RT-PCR. These were 6-OST1 FP2: CTGCATCTTCTTACCCTTTAC; 6-OST2 FP3: GGTCAGAATCTGAGTCAGAATC; 6-OST3 RP2: CCAAAGTAATCCAAGAGAAG.

To confirm amplification specificity, the PCR products from each primer pair for each run were subjected to melting curve analysis subsequent to real-time amplification. In addition, a standard PCR reaction (no SYBR Green, 2 µl cDNA as template) was run in parallel with each real-time run, and the products were subjected to agarose gel electrophoresis. The relative quantification as determined through fluorescence was always closely reflected by the relative intensity of UV-visualized bands on the gel. Each real-time run consisted of a series of six standards to generate the standard curve used to quantify cDNA samples in addition to the series of cDNA samples being tested. Standard curves for the OSTs were prepared as follows. The products amplified by each set of primers for 2-OST, 6-OST1, 6-OST2, and 6-OST3 were purified using a Concert PCR product purification kit (Invitrogen) according to the manufacturer's instructions. Products were quantified spectrophotometrically and 10-fold dilutions were prepared in Tris-EDTA buffer (pH 7.5) ranging from 100,000 pg/ml to 1 pg/ml. Two microliters of each standard was used per PCR reaction for real-time quantification as described.

Table I. Parameters for real-time quantitative RT-PCR data acquisition on HS-OSTs

HS OST	Primers	T_{anneal}	Mg^{2+} (mM)	T_{melt} (Tm)	$T_{acquire}$	PCR product (bp)
2-OST	RP1 and FP1	55	2	91	87	570
6-OST1	FP2 and RP1	55	2	91	87	350
6-OST2	FP3 and RP1	55	3	90	87	368
6-OST3	FP1 and RP2	55	3	90	87	501

Semi-quantitative RT-PCR of FGFR b and c splice variant expression

The methodology for both cDNA synthesis and subsequent PCR were essentially as already described. The FGFR splice variant RT-PCR strategy used primers as follows.
Forward for loop III PCR:
- FGFR1b, CTTGACGTCGTGGAACGATCT;
- FGFR1c, CTTGACGTCGTGGAACGATCT;
- FGFR2b, CCCATCCTCCAAGCTGGACTGCCT;
- FGFR2c, CCCATCCTCCAAGCTGGACTGCCT;
- FGFR3b GACATACACACTGGATGTGCTGGA;
- FGFR3c, GACATACACACTGGATGTGCTGGA;
- FGFR4, CAACTCCATCGGCCTTTCCTACCA.

Reverse (for Loop III cDNA synthesis and PCR):
- FGFR1b, CTGGTTAGCTTCACCAATAT;
- FGFR1c, TTCCAGAACGGTCAACCATGCAGA;
- FGFR2b, ATCTGGGGAAGCCGTGATCTCCTT;
- FGFR2c, TGGCAGAACTGTCAACCATGCAGA;
- FGFR3b, GGCCTTCTCAGCCACGCCTAT;
- FGFR3c, AGCACCACCAGCCACGCAGAGTGA;
- FGFR4, GGCAGGTCTAGATTCACAAGGCCC.

Internal (5′, for exon-specific PCR):
- FGFR1b, CGGGAATTAATAGCTCGGAT;
- FGFR1c, ACTGCTGGAGTTAATACCACCGAC;
- FGFR2b, CTGAAGCACTCGGGGATAAATAGC;
- FGFR2c, GGTGTTAACACCACGGACAAAGAG;
- FGFR3b, GAATGTGGAGGCAGACGCACG;
- FGFR3c, TGCAGGCGCTAACACCACCGACAA;
- FGFR4, CAGGCTCACTGGTTCTGCTTGTGC.

The design allows for RT-PCR expression analysis of the b or c splice variant using the Loop III forward and reverse primers and for subsequent Southern analysis of the PCR products for verification of identity using the internal 5′ b or c exon-specific primers as probes. PCR products were transferred to a Hybond N+ (Amersham) membrane and hybridized at 42°C overnight with their corresponding internal primers that had been end-labeled with γ-^{32}P-ATP and polynucleotide kinase (Southern conditions and end-labeling detailed in Ford *et al.*, 1997). To quantify the expression levels of each gene the intensities of the PCR product bands at 30 cycles were measured by exposing the blots to a PhosphorImager screen (Fujix Imaging Plate, Type BAS-IIIS) and using MacBasII software. Analyses were performed in duplicate on duplicate RNA preparations from the different ages and signals quantified using a Fujix PhosphorImager and MacBasII software. The results represent mean values ± SD.

HS purification and BaF3 assays

HS was purified from primary cultures of Nep cells as described (Brickman *et al.*, 1998a,b). BaF3 lymphoid cells expressing various FGFR isoforms (Ornitz *et al.*, 1996) were incubated for 72 h with 1 nM FGF1, FGF2, or FGF8 (b isoform) and HS from $E10^{+2}$ or $E12^{+2}$ cells. Cell numbers were measured using an MTT (3-[4,5-Dimethylthiazol-2-yl]-2,5 diphenyltetrazolium bromide) assay as described (Guimond and Turnbull, 1999). Data is presented as mean ± SD.

Acknowledgments

We thank Dave Ornitz (University of St. Louis) for BaF3 cell lines and Clive Dickson (ICRF, London) for FGF8. This work is supported by grants from the Medical Research Council, UK (senior research fellowship to J.E.T.); the Royal Society (travel grant to S.E.G); National Health and Medical Research Council of Australia (M.F.-P. and M.M.); National Institutes of Health grant R37GM33063 (J.D.E.); Deutsche Forschungsgemeinschaft Grant GR-1748 (K.G.); Aichi Medical University (K.K. and H.H) and the Ministry of Education, Science, Sport, and Culture of Japan (K.K. and H.H.).

Abbreviations

E(10), embryonic day (10); FGF, fibroblast growth factor; FGFR, fibroblast growth factor receptor; HS, heparan sulfate; HSPG, heparan sulfate proteoglycan; HSST, heparan sulfate sulfotransferase; NDST, N-deacetylase-N-sulfotransferase; Nep, neural precursor; OST, O-sulfotransferase; RT-PCR, reverse transcription polymerase chain reaction.

References

Aikawa, J., Grobe, K., Tsujimoto, M., and Esko, J.D. (2001) Multiple isozymes of heparan sulfate/heparin GlcNAc N-deacetylase/GlcN N-sulfotransferase. Structure and activity of the fourth member, NDST4. *J. Biol. Chem.*, **276**, 5876–5882.

Allen, B.L., Filla, M.S., and Rapraeger, A.C. (2001) Role of heparan sulfate as a tissue-specific regulator of FGF-4 and FGF receptor recognition. *J. Cell Biol.*, **155**, 845–858.

Bernfield, M., Gotte, M., Park, P.W., Reizes, O., Fitzgerald, M.L., Lincecum, J., and Zako, M. (1999) Functions of cell surface heparan sulfate proteoglycans. *Annu. Rev. Biochem.*, **68**, 729–777.

Brickman, Y.G., Ford, M.D., Gallagher, J.T., Nurcombe, V., Bartlett, P.F., and Turnbull, J.E. (1998a) Structural modification of fibroblast growth factor-binding heparan sulfate at a determinative stage of neural development. *J. Biol. Chem.*, **273**, 4350–4359.

Brickman, Y., Ford, M., Gallagher, J., Nurcombe, V., Bartlett, P., and Turnbull, JE. (1998b) Structural comparison of FGF-specific heparan sulfates derived from a growing or differentiating neuroepithelial cell line. *Glycobiology*, **8**, 463–471.

Bullock, S.L., Fletcher, J.M., Beddington, R.S., and Wilson, V.A. (1998) Renal agenesis in mice homozygous for a gene trap mutation in the gene encoding heparan sulfate 2-sulfotransferase. *Genes Dev.*, **12**, 1894–1906.

Caviness, V.S. Jr., Takahashi, T., and Nowakowski, R.S. (1995) Numbers, time and neocortical neuronogenesis: a general developmental and evolutionary model. *Trends Neurosci.*, **18**, 379–383.

Crossley, P.H., Martinez, S., and Martin, G.R. (1996) Midbrain development induced by FGF8 in the chick embryo. *Nature*, **380**, 66–68.

Ford, M.D., Cauchi, J., Greferath, U., and Bertram, J.F. (1997) Expression of fibroblast growth factors and their receptors in rat glomeruli. *Kidney Int.*, **51**, 1729–1738.

Ford-Perriss, M., Abud, H., and Murphy, M. (2001) Fibroblast growth factors in the developing central nervous system. *Clin. Exp. Pharmacol. Physiol.*, **28**, 493–503.

Forsberg, E., Pejler, G., Ringvall, M., Lunderius, C., Tomasini-Johansson, B., Kusche-Gullberg, M., Eriksson, I., Ledin, J., Hellman, L., and Kjellen, L. (1999) Abnormal mast cells in mice deficient in a heparin-synthesizing enzyme. *Nature*, **400**, 773–776.

Fukuchi-Shimogori, T. and Grove, E.A. (2001) Neocortex patterning by the secreted signaling molecule FGF8. *Science*, **294**, 1071–1074.

Grobe, K. and Esko, J. (2002) Regulated translation of heparan sulphate GlcNAc N-Deacetylase/N-sulfotransferase isozymes by structured 5[1]-untranslated regions and internal ribosome entry sites. *J. Biol. Chem.,* forthcoming.

Guimond, S.E. and Turnbull, J.E. (1999) Fibroblast growth factor receptor signaling is dictated by specific heparan sulfate saccharides. *Curr. Biol.*, **9**, 1343–1346.

Guimond, S., Maccarana, M., Olwin, B.B., Lindahl, U., and Rapraeger, A.C. (1993) Activating and inhibitory heparin sequences for FGF-2 (basic FGF). Distinct requirements for FGF-1, FGF-2, and FGF-4. *J. Biol. Chem.*, **268**, 23906–23914.

Habuchi, H., Tanaka, M., Habuchi, O., Yoshida, K., Suzuki, H., Ban, K., and Kimata, K. (2000) The occurrence of three isoforms of heparan sulfate 6-O-sulfotransferase having different specificities for hexuronic acid adjacent to the targeted N-sulfoglucosamine. *J. Biol. Chem.*, **275**, 2859–2868.

Humphries, D.E., Wong, G.W., Friend, D.S., Gurish, M.F., Qiu, W.T., Huang, C., Sharpe, A.H., and Stevens, R.L. (1999) Heparin is essential for the storage of specific granule proteases in mast cells. *Nature*, **400**, 769–772.

Kan, M., Wu, X., Wang, F., and McKeehan, W.L. (1999) Specificity for fibroblast growth factors determined by heparan sulfate in a binary complex with the receptor kinase. *J. Biol. Chem.*, **274**, 15947–15952.

Kobayashi, M., Habuchi, H., Yoneda, M., Habuchi, O., and Kimata, K. (1997) Molecular cloning and expression of Chinese hamster ovary cell heparan-sulfate 2-sulfotransferase. *J. Biol. Chem.*, **272**, 13980–13985.

Lander, A.D. and Selleck, S.B. (2000) The elusive functions of proteoglycans: *in vivo* veritas. *J. Cell Biol.*, **148**, 227–232.

Lindahl, U., Kusche-Gullberg, M., and Kjellen, L. (1998) Regulated diversity of heparan sulfate. *J. Biol. Chem.*, **273**, 24979–24982.

Liu, J., Shworak, N., Sinay, P., Schwartz, J., Zhang, L., Fritze, L., and Rosenberg, R. (1999) Expression of heparan sulfate D-glucsaminyl 3-O-sulfotransferase isoforms reveals novel substrate specificities. *J. Biol. Chem.*, **274**, 5185–5192.

Martinez, S., Crossley, P.H., Cobos, I., Rubenstein, J.L., and Martin, G.R. (1999) FGF8 induces formation of an ectopic isthmic organizer and isthmocerebellar development via a repressive effect on Otx2 expression. *Development*, **126**, 1189–1200.

Murphy, M., Drago, J., and Bartlett, P.F. (1990) Fibroblast growth factor stimulates the proliferation and differentiation of neural precursor cells *in vitro*. *J. Neurosci. Res.*, **25**, 463–475.

Murphy, M., Reid, K., Ford, M., Furness, J.B., and Bartlett, P.F. (1994) FGF2 regulates proliferation of neural crest cells, with subsequent neuronal differentiation regulated by LIF or related factors. *Development*, **120**, 3519–3528.

Ornitz, D.M. (2000) FGFs, heparan sulfate and FGFRs: complex interactions essential for development. *Bioessays*, **22**, 108–112.

Ornitz, D.M., Xu, J., Colvin, J.S., McEwen, D.G., MacArthur, C.A., Coulier, F., Gao, G., and Goldfarb, M. (1996) Receptor specificity of the fibroblast growth factor family. *J. Biol. Chem.*, **271**, 15292–15297.

Orr-Urtreger, A., Givol, D., Yayon, A., Yarden, Y., and Lonai, P. (1991) Developmental expression of two murine fibroblast growth factor receptors, flg and bek. *Development*, **113**, 1419–1434.

Pikas, D.S., Eriksson, I., and Kjellen, L. (2000) Overexpression of different isoforms of glucosaminyl N-deacetylase/N-sulfotransferase results in distinct heparan sulfate N-sulfation patterns. *Biochemistry*, **39**, 4552–4558.

Pye, D.A., Vives, R.R., Hyde, P., and Gallagher, J.T. (2000) Regulation of FGF-1 mitogenic activity by heparan sulfate oligosaccharides is dependent on specific structural features: differential requirements for the modulation of FGF-1 and FGF-2. *Glycobiology*, **10**, 1183–1192.

Qian, X., Davis, A.A., Goderie, S.K., and Temple, S. (1997) FGF2 concentration regulates the generation of neurons and glia from multipotent cortical stem cells. *Neuron*, **18**, 81–93.

Raballo, R., Rhee, J., Lyn-Cook, R., Leckman, J.F., Schwartz, M.L., and Vaccarino, F.M. (2000) Basic fibroblast growth factor (Fgf2) is necessary for cell proliferation and neurogenesis in the developing cerebral cortex. *J. Neurosci.*, **20**, 5012–5023.

Ragsdale, C.W.and Grove, E.A. (2001) Patterning the mammalian cerebral cortex. *Curr. Opin. Neurobiol.*, **11**, 50–58.

Ringvall, M., Ledin, J., Holmborn, K., van Kuppevelt, T., Ellin, F., Eriksson, I., Olofsson, A.M., Kjellen, L., and Forsberg, E. (2000) Defective heparan sulfate biosynthesis and neonatal lethality in mice lacking N-deacetylase/N-sulfotransferase-1. *J. Biol. Chem.*, **275**, 25926–25930.

Shimamura, K. and Rubenstein, J.L. (1997) Inductive interactions direct early regionalization of the mouse forebrain. *Development*, **124**, 2709–2718.

Shworak, N.W., Liu, J., Petros, L.M., Zhang, L., Kobayashi, M., Copeland, N.G., Jenkins, N.A., and Rosenberg, R.D. (1999) Multiple isoforms of heparan sulfate D-glucosaminyl 3-O-sulfotransferase. Isolation, characterization, and expression of human cdnas and identification of distinct genomic loci. *J. Biol. Chem.*, **274**, 5170–5184.

Turnbull, J., Powell, A., and Guimond, S. (2001) Heparan sulfate: decoding a dynamic multifunctional cell regulator. *Trends Cell. Biol.*, **11**, 75–82.

Vaccarino, F.M., Schwartz, M.L., Raballo, R., Nilsen, J., Rhee, J., Zhou, M., Doetschman, T., Coffin, J.D., Wyland, J.J., and Hung, Y.T. (1999) Changes in cerebral cortex size are governed by fibroblast growth factor during embryogenesis. *Nat. Neurosci.*, **2**, 246–253.

Wuechner, C., Nordqvist, A.C., Winterpacht, A., Zabel, B., and Schalling, M. (1996) Developmental expression of splicing variants of fibroblast growth factor receptor 3 (FGFR3) in mouse. *Int. J. Dev. Biol.*, **40**, 1185–1188.